https://doi.org/10.5194/hess-2022-309
Preprint. Discussion started: 15 September 2022

Hydrology and Earth System Sciences
Discussions

An analytical generalization of Budyko framework with physical accounts of climate seasonality and water storage capacity

Xu Zhang [1], Jinbao Li [1], Qianjin Dong [2], Ross A. Woods [3]

[1] Department of Geography, University of Hong Kong, Hong Kong SAR, China
[2] State Key Laboratory of Water Resources and Hydropower Engineering Science, Wuhan University, Wuhan, China
[3] Department of Civil Engineering, University of Bristol, Bristol, UK

Correspondence to: Xu Zhang (zhangxu_hku@connect.hku.hk)

Abstract. The Budyko framework is an effective and widely used method for describing long-term water balance in large catchments. However, it only considers the limits of water and energy in evaporation (E), and ignores the impacts of climate seasonality and water storage capacity (S_c), resulting in errors for Mediterranean climate and catchments with small S_c. Here we combined the Ponce-Shetty model with Budyko hypothesis, and analytically generalized Budyko framework with physical accounts of climate seasonality and S_c. Precipitation (P), potential evaporation (PE), and S_c are used to represent the limits of water, energy, and space for E, respectively. Our results show that previous Budyko-type equations can be treated as special cases of generalized Budyko-type equations with uniform P and PE and infinite S_c. The new generalized equations capture the observed decrease in E due to asynchronous P and PE and small S_c, and perform better than the Budyko-type equations with varying parameters in the contiguous United States with fewer parameters. Overall, our generalization of Budyko framework improves the robustness and accuracy for estimating mean annual E with the aid of physical interpretation, and will facilitate water balance assessment at regional to global scales.

1 Introduction

Accurate description of the balance between precipitation (P), evaporation (E), and runoff (R) is a key issue in climatology, hydrology, ecology, and many related fields (Milly et al., 2005; Vörösmarty et al., 2010; Oki and Kanae, 2006). A large number of theories and models have been devised to simulate water cycles for different climates at various timescales (Arnold et al., 1998; Henley et al., 2011; Lan et al., 2018; Martinez and Gupta, 2010; Westra et al., 2014; Zhang et al., 2020). However, due to the complexity and spatial variety in global catchments, hydrological models generally require some parameters and observational data for calibration, which are valid only in certain regions and hamper their applications at a global scale (Beven, 1993; Moretti and Montanari, 2007; Arnold et al., 1998).

Among the water balance models, the Budyko framework is unique in that it has a very simple structure with minimal data inputs but achieves good performance worldwide (Mianabadi et al., 2020; Berghuijs et al., 2020). In this framework, only water and energy limits of E are assumed over the long-term period for large catchments (Mianabadi et al., 2020;

Hydrology and Earth System Sciences
Open Access
EGU
Discussions

Budyko, 1974; Fu, 1981; Wang and Tang, 2014). With available water measured by P and energy represented by potential evaporation (PE), the boundary conditions of E can be derived in extreme wet and dry climates, which underpin various derivations of Budyko-type equations (Budyko, 1974; Fu, 1981; Yang et al., 2008; Wang and Tang, 2014; Zhang et al., 2004). Besides that, Zhou et al. (2015b) proposed a function $g(\emptyset)$ that can systematically unify the theoretical derivations of Budyko-type equations from the boundary conditions. Till now, the Budyko-type equations have been widely employed in the studies of climate sensitivity (Gudmundsson et al., 2016; Wu et al., 2017; Berghuijs et al., 2017; Liu et al., 2020; Zhou et al., 2015a), runoff simulation (Zhang et al., 2008; Zhang et al., 2020; Gao et al., 2020), decomposition of runoff change (Wang and Hejazi, 2011; Zhang et al., 2019b), land-runoff interaction (Yang et al., 2007; Yang et al., 2009; Istanbulluoglu et al., 2012; Ning et al., 2019), among others (Greve et al., 2020; Berghuijs et al., 2014).

Despite the wide applications of Budyko-type equations, the departure of the simulated E from observations is still hard to explain (Wu et al., 2018b; Mianabadi et al., 2020). Many studies attribute the departure to the synthesized parameter (ω or n) in one-parameter Budyko-type equations, assuming that the synthesized parameter represents all catchment properties except for aridity index ($\frac{PE}{P}$) (Gudmundsson et al., 2016; Zhang et al., 2019a; Berghuijs et al., 2017; Istanbulluoglu et al., 2012). Factors like soil properties, vegetation cover, precipitation seasonality, human water consumption are regressed to the synthesized parameter (Jiang et al., 2015; Zhang et al., 2019a; Zhang et al., 2019b; Yang et al., 2007; Yang et al., 2009; Li et al., 2013). However, no consensus has been achieved on the controlling factors of ω (Greve et al., 2015; Zhou et al., 2015b; Mianabadi et al., 2020), suggesting that a synthesized parameter may not be capable of representing all the catchment properties due to its unclear physical interpretation (Reaver et al., 2022).

Compared to hydrological models operating on daily or monthly timescales, the Budyko-type equations do not consider climate seasonality and underlying surface conditions. Previous studies find that mean annual E in the catchments with synchronous (asynchronous) P and PE is systematically underestimated (overestimated) by Budyko-type equations (Berghuijs et al., 2020; De Lavenne and Andréassian, 2018; Potter et al., 2005). Water storage capacity plays a significant role in long-term hydrological balance from analytical derivation and may control the errors in Budyko framework (Milly, 1994; Woods, 2003; Daly et al., 2019; Rodriguez-Iturbe et al., 1999; Sivapalan et al., 2011; Milly, 1993; Bondy et al., 2021; Wu et al., 2018a). As documented by Rodriguez-Iturbe et al. (1999) and Daly et al. (2019), if a catchment has a very small water storage capacity or asynchronous P and PE, the R will be generated and flow out of the catchment soon after precipitation falls onto land surface. Under this circumstance, there is not much space and time for evaporation, and the E will be close to 0 regardless of P or PE. Therefore, Budyko-type equations, which only use mean annual aridity index ($\frac{PE}{P}$) as an explanatory variable, may induce large errors, and are available only for very large catchments having similar climate seasonality and water storage capacity. A theoretical improvement to Budyko framework with physical accounts of climate seasonality and water storage capacity is imperative.

The main objective of this study is to analytically generalize the Budyko framework in order to physically incorporate climate seasonality and water storage capacity. A new variable that is measured from soil properties will be included in E

https://doi.org/10.5194/hess-2022-309
Preprint. Discussion started: 15 September 2022

Hydrology and Earth System Sciences Discussions

estimation to represent water storage capacity. Hydrological processes are simulated at a sub-annual timescale to consider climate seasonality. The new generalized Budyko-type equations will be tested against 471 catchments in the contiguous United States (CONUS) to assess their physical interpretation and performance. The results are expected to improve our physical understanding of water cycles and the interplay between hydrological and climatic conditions.

2 Analytical generalization of Budyko framework

The analytical generalization of Budyko framework is achieved through the conceptualization of E, Ponce-Shetty model, and its formulation using Budyko-type equations. In the following, conceptualization of mean annual E generation is first introduced to present timescales and some assumptions in runoff generation (Section 2.1). The two partitioning stages in Ponce-Shetty model are then provided to give the relationships and boundary conditions between hydrological variables (Section 2.2). The Budyko-type equations are used as tools for formulating E in Ponce-Shetty model (Section 2.3). Lastly, the generalized Budyko-type equations are derived from the outputs of two stages (Section 2.4).

2.1 Conceptualization of mean annual E generation

In the conceptualization of E generation, inter-annual variations between hydrological variables are assumed to be zero as the derivations of previous long-term water balance equations (Wang and Tang, 2014; Yang et al., 2008; Fu, 1981). The main objective of generalized Budyko equation is to depict the spatial variability of mean annual E for multiple catchments. Despite the negligible inter-annual variations, intra-annual variations in P and PE are necessary to be included given the essential role of climate seasonality in controlling errors in Budyko framework (Berghuijs et al., 2020; De Lavenne and Andréassian, 2018). Thus, hydrological year (starting from 1st, Oct.) used in this study is divided into three time intervals with a length of 4 months, and E in each 4-month time interval is modeled using Ponce-Shetty model. Water storage is assumed to be depleted at the end of each time interval following previous analytical derivation (Rodriguez-Iturbe et al., 1999; Porporato et al., 2004; Daly et al., 2019; Sankarasubramanian and Vogel, 2002). The assumption of 4-month timescale is based on the rising-recession-depletion period in hydrograph and baseflow recession curves, which ranges from 90 to 150 days (Yang et al., 2018; Vitvar et al., 2002; Dunn et al., 2007; Katsuyama et al., 2010). Thus, rainfall may need approximately 4 months to generate surface runoff, infiltrate in the soil, pass the aquifer, and reach catchment outlet before catchment water storage is negligible, indicating a complete rainfall-runoff event may take 4 months. Meanwhile, Ponce-Shetty model only assumes one complete rainfall-runoff event with zero water storage change for E estimation (Ponce and Shetty, 1995; L′Vovich, 1979), and therefore was applied at the 4-month timescale.

To sum up, mean annual hydrological processes are assumed to consist of three complete rainfall-runoff events. Each event lasts for four months, and is modeled by Ponce-Shetty model. Other timescales are further examined and discussed in Section 5. Herein, mean 4-month variables are denoted by subscript j ($j = 1$ for Oct.-Jan., $j = 2$ for Feb.- May, $j = 3$ for Jun.- Sep.), and mean annual values are denoted by subscript a. Mean 4-month and mean annual P, PE, and E are the

https://doi.org/10.5194/hess-2022-309
Preprint. Discussion started: 15 September 2022

Hydrology and Earth System Sciences
Discussions
Open Access

products of mean water fluxes and associated timescales (i.e., 4 months or one year), and share a unit of millimeter (mm) in this study.

2.2 Ponce-Shetty model

Ponce-Shetty model is a water balance model with numerous applications worldwide (Gnann et al., 2019; Sivapalan et al., 2011), and is used here to formulate E_j in each 4-month time interval. Two partitioning stages are assumed for fast flow and baseflow, respectively (Wang et al., 2015; Zhao et al., 2016; Ponce and Shetty, 1995; L′Vovich, 1979), and boundary relationships are introduced as follows.

2.2.1 The first partitioning stage

The first stage in the Ponce-Shetty model describes the partitioning of P_j into fast flow ($Q_{f,j}$) and wetting (W_j) as follows (Figure 1a)

$$P_j = Q_{f,j} + W_j \tag{1}$$

$$1 = \frac{Q_{f,j}}{P_j} + \frac{W_j}{P_j} \tag{2}$$

where W_j represents the amount of water stored in the catchment for second partitioning stage. W_j is limited by two factors. The first is P_j, which measures available atmospheric input water. The second is water storage capacity (S_c), which represents the maximum volume of water that can be saved in the catchment, and is measured from observed soil porosity and soil depth in this study.

The boundary conditions of W_j are derived from the catchments with extreme P_j and S_c. For the catchments with infinite atmospheric input water ($P_j \to +\infty$) or infinitesimal storage capacity ($S_c \to 0$), atmospheric input water is much greater than the space that can be used for storing water ($\frac{S_c}{P_j} \to 0$). Thus, nearly all spaces that can be used for storing water, measured as S_c, are filled up, while P_j is still large enough to provide sufficient atmospheric input water much greater than S_c (Figure 1b). Under this circumstance, S_c mainly limits W_j, and W_j approach to S_c.

$$W_j \to S_c, as\ \frac{S_c}{P_j} \to 0 \tag{3}$$

Furthermore, we can derive that $\frac{W_j}{P_j} \to 0$ because $W_j < S_c$ and $\frac{W_j}{P_j} < \frac{S_c}{P_j} \to 0$. Combined it with Eq. (2), we can obtain that $\frac{Q_{f,j}}{P_j}$ approaches 1.

$$\frac{Q_{f,j}}{P_j} = 1 - \frac{W_j}{P_j} \to 1, as\ \frac{S_c}{P_j} \to 0 \tag{4}$$

For the catchments with infinitesimal input water ($P_j \rightarrow 0$) or infinite storage capacity ($S_c \rightarrow +\infty$), atmospheric input water is much less than the space that can be used for storing water ($\frac{S_c}{P_j} \rightarrow +\infty$). Nearly all P_j will be stored in the catchments, and S_c is still large enough to store much more water (Figure 1c). Thus, P_j mainly limits W_j, and W_j approach to P_j.

$$W_j \rightarrow P_j, as\ \frac{S_c}{P_j} \rightarrow +\infty \quad (5)$$

We can obtain that $\frac{W_j}{P_j} \rightarrow 1$ based on $W_j \rightarrow P_j$ in the above equation. Thus, $\frac{Q_{f,j}}{P_j}$ approaches 0 in the combination with Eq. (2).

$$\frac{Q_{f,j}}{P_j} = 1 - \frac{W_j}{P_j} \rightarrow 0, as\ \frac{S_c}{P_j} \rightarrow +\infty \quad (6)$$

2.2.2 The second partitioning stage

In the second stage, W_j is further partitioned into baseflow ($Q_{b,j}$) and evaporation (E_j) (Figure 1d).

$$W_j = Q_{b,j} + E_j \quad (7)$$

$$1 = \frac{Q_{b,j}}{W_j} + \frac{E_j}{W_j} \quad (8)$$

The E_j is also limited by two factors. The first is W_j, which measures the amount of water that is stored in the catchment after the first partitioning stage and represents available water to be evaporated. The second limiting factor is the PE_j, which measures the atmospheric demand and represents available energy that can transform liquid water into water vapor.

Similarly, the boundary conditions of the second partitioning stage can be derived from the catchments with extreme PE_j and W_j. For the catchments with infinite atmospheric demand ($PE_j \rightarrow +\infty$) or infinitesimal water storage ($W_j \rightarrow 0$), atmospheric demand is much greater than the water that is stored in the catchment ($\frac{PE_j}{W_j} \rightarrow +\infty$). Thus, nearly all available water stored in the catchments, measured as W_j, will be evaporated into the atmosphere, while PE_j is still large enough to evaporate much more water than W_j (Figure 1e). The W_j mainly limits E_j, and E_j approach to W_j.

$$E_j \rightarrow W_j, as\ \frac{PE_j}{W_j} \rightarrow +\infty \quad (9)$$

It can be obtained that $\frac{E_j}{W_j} \rightarrow 1$ based on $E_j \rightarrow W_j$ in the above equation. Thus, $\frac{Q_{b,j}}{W_j}$ approaches to 0 from Eq. (8).

https://doi.org/10.5194/hess-2022-309
Preprint. Discussion started: 15 September 2022

Hydrology and Earth System Sciences
Discussions

$$\frac{Q_{b,j}}{W_j} = 1 - \frac{E_j}{W_j} \to 0, as\ \frac{PE_j}{W_j} \to +\infty \tag{10}$$

For the catchments with infinitesimal atmospheric demand ($PE_j \to 0$) or infinite water storage ($W_j \to +\infty$), atmospheric demand is much less than the water that is stored in the catchment ($\frac{PE_j}{W_j} \to 0$). Thus, atmospheric demand, measured as PE_j, can be easily fulfilled, and W_j is still sufficient to supply much more water than PE_j (Figure 1f). The PE_j mainly limits E_j, and E_j approach to PE_j.

$$E_j \to PE_j, as\ \frac{PE_j}{W_j} \to 0 \tag{11}$$

It can be obtained that $\frac{E_j}{W_j} \to 0$ because $E_j < PE_j$ and $\frac{E_j}{W_j} < \frac{PE_j}{W_j} \to 0$. The $\frac{Q_{b,j}}{W_j}$ approaches 1 from Eq. (8)

$$\frac{Q_{b,j}}{W_j} = 1 - \frac{E_j}{W_j} \to 1, as\ \frac{PE_j}{W_j} \to 0 \tag{12}$$

In summary, two partitioning stages were assumed for E_j from the Ponce-Shetty model, and the boundary conditions are analytically derived. Eqs. (3) to (6) are the boundary conditions for the first partitioning under $\frac{W_P}{P_j} \to 0$ or $\frac{W_P}{P_j} \to +\infty$. Eqs. (9) to (12) are the boundary conditions of the second partitioning when $\frac{PE_j}{W_j} \to 0$ or $\frac{PE_j}{W_j} \to +\infty$.

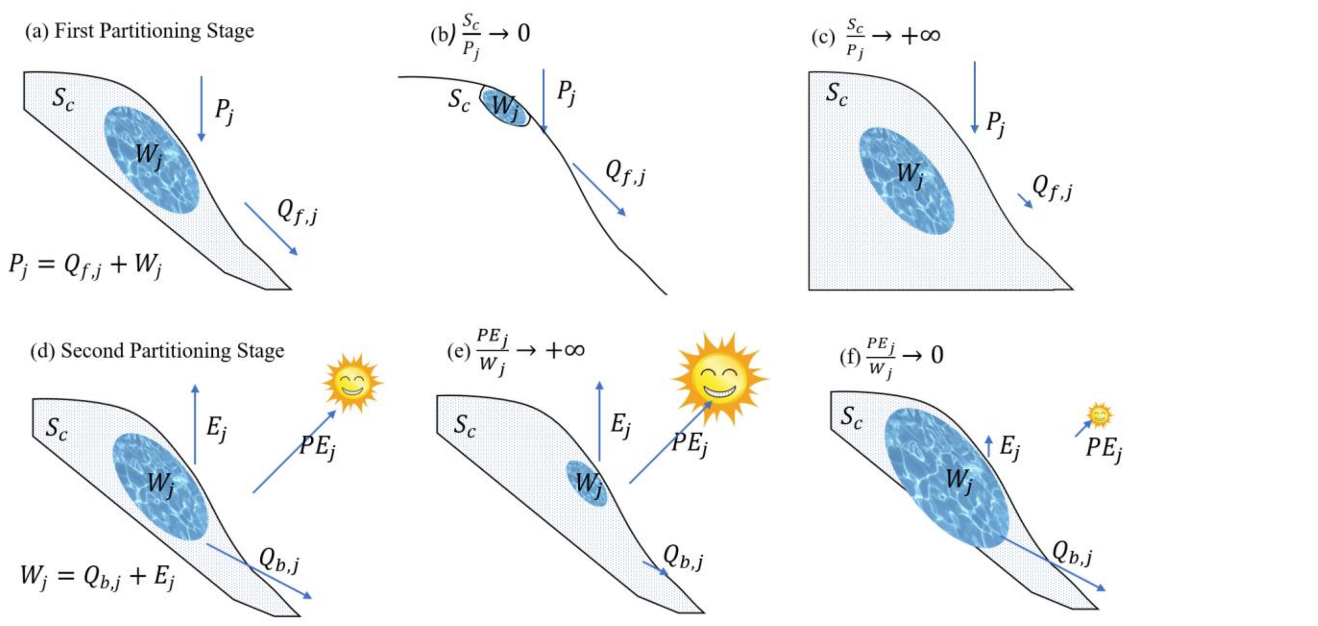

Figure 1 Schematic of the Ponce-Shetty model. (a-c) The first partitioning stage (a) and its related boundary conditions (b and c). (d-f) The second partitioning stage (d) and its related boundary conditions (e and f).

https://doi.org/10.5194/hess-2022-309
Preprint. Discussion started: 15 September 2022

2.3 Modeling of the two partitioning stages using Budyko framework

The two partitioning stages in the Ponce-Shetty model were originally modeled using proportionality hypothesis with four parameters (Ponce and Shetty, 1995; L'Vovich, 1979). Recent studies have shown that proportionality hypothesis shares the same boundary conditions as the Budyko-type equations (Zhang et al., 2020; Wang and Tang, 2014; Wang et al., 2015; Zhao et al., 2016), indicating that Budyko-type equations are capable of modeling variables in Ponce-Shetty model. We introduce the capability of Budyko-type equations in Section 2.3.1, and then replace the proportionality hypothesis with Budyko hypothesis to model two partitioning stage in Section 2.3.2.

2.3.1 Capability of Budyko-type equations

Budyko-type equations are derived based on the supply and demand limits, and are capable of modeling the variables with following relationships (Zhou et al., 2015b)

$$Z = \mathrm{X} + \mathrm{Y} \tag{13}$$

$$X \to X_{max}, as\ \frac{X_{max}}{Z} \to 0 \tag{14}$$

$$X \to \mathrm{Z}, as\ \frac{X_{max}}{Z} \to +\infty \tag{15}$$

where X_{max} is the potential maximum value of X due to external factors. Quantities Z and X_{max} are derived from observations, and X can be simulated using Budyko-type equations as

$$X = B(Z, X_{max}, n) \tag{16}$$

where $B(\,)$ is a one-parameter Budyko-type equation. The inclusion of a synthesized parameter (n) provides the flexibility for capturing other factors apart from Z and X_{max}. Here, two analytically-derived one-parameter Budyko-type equations, including the Yang equation (Yang et al., 2008) and Fu equation (Fu, 1981; Zhang et al., 2004), are provided for $B(\,)$ and listed in Table 1.

2.3.2 Modeling of two partitioning stages

By comparing the boundary conditions in the first partitioning stage (i.e., Eqs (3) to (6)) with Eqs. (13) to (15), we find that P_j, W_j, $Q_{f,j}$, and S_c share the same boundary conditions as Z, X, Y, and X_{max}. Thus, the one-parameter Budyko-type equations can be used to model the first partitioning as

$$W_j = B_1(P_j, S_c, n_1) \tag{17}$$

where $B_1(\,)$ is a Budyko-type equation that models the first partitioning stage, and n_1 is a synthesized parameter controlling the first partitioning except P_j and S_c.

https://doi.org/10.5194/hess-2022-309
Preprint. Discussion started: 15 September 2022

Similarly, the boundary conditions of W_j, E_j, $Q_{b,j}$, and PE_j in the second partitioning stage (i.e., Eqs (9) to (12)) share the same forms as Z, X, Y, and X_{max} (i.e., Eqs. (13) to (15)). Thus, the second partitioning can also be modeled using Budyko-type equations

$$E_j = B_2(W_j, PE_j, n_2) \tag{18}$$

where $B_2(\,)$ is a Budyko-type equation for the second partitioning stage, n_2 is the second synthesized parameter controlling the second partitioning except PE_j and W_j.

2.4 Generalized Budyko-type equations for E_a

After the modeling of two partitioning stages, E_j can be obtained by replacing W_j in Eq. (18) with Eq. (17).

$$E_j = B_2(B_1(P_j, S_c, n_1), PE_j, n_2) \tag{19}$$

Mean annual evaporation (E_a) can be expressed as the sum of E_j in three 4-month time intervals during a hydrological year.

$$E_a = \sum_{j=1}^{3} E_j = \sum_{j=1}^{3} B_2(B_1(P_j, S_c, n_1), PE_j, n_2) \tag{20}$$

Eq. (20) is the generalized Budyko-type equation and is rewritten as follows for visualization

$$E_a = \sum_{j=1}^{3} f_g(P_j, PE_j, S_c, n_1, n_2) \tag{21}$$

In the generalized equations, E_a is jointly controlled by three explanatory variables, including P_j, PE_j, and S_c, representing the limits of water, energy, and space, respectively. Two parameters, n_1 and n_2, are incorporated to control two stages. The sum of 4-month E_j allows the generalized equations to incorporate climate seasonality at a 4-month resolution. The combination of two Budyko-type equations, including Fu and Yang equations, generates four generalized Budyko-type equations (Table 1).

Table 1 Expressions of two one-parameter Budyko-type equations and their generalized Budyko-type equations.

Type	Name	Expression
Budyko-type equation	Yang equation	$X = (Z^{-n} + {X_{max}}^{-n})^{-\frac{1}{n}}, n > 0$
	Fu equation	$X = Z + X_{max} - (Z^n + {X_{max}}^{n})^{\frac{1}{n}}, n > 1$
Generalized Budyko-type equations	Yang -Yang	$E_a = \sum_{j=1}^{3}(((P_j^{-n_1} + S_c^{-n_1})^{-\frac{1}{n_1}})^{-n_2} + PE_j^{-n_2})^{-\frac{1}{n_2}}$
	Yang -Fu	$E = \sum_{j=1}^{3}(P_j^{-n_1} + S_c^{-n_1})^{-\frac{1}{n_1}} + PE_j - \left(((P_j^{-n_1} + S_c^{-n_1})^{-\frac{1}{n_1}})^{n_2} + PE_j^{n_2}\right)^{\frac{1}{n_2}}$

Fu - Yang	$E_a = \sum_{j=1}^{3}((P_j + S_c - (P_j^{n_1} + S_c^{n_1})^{\frac{1}{n_1}})^{-n_2} + PE_j^{-n_2})^{-\frac{1}{n_2}}$
Fu - Fu	$E_a = \sum_{j=1}^{3} P_j + S_c - (P_j^{n_1} + S_c^{n_1})^{\frac{1}{n_1}} + PE_j - \left((P_j + S_c - (P_j^{n_1} + S_c^{n_1})^{\frac{1}{n_1}})^{n_2} + PE_j^{n_2}\right)^{\frac{1}{n_2}}$

3 Properties of the generalized Budyko-type equations

3.1 Proportional relationship

The generalized Budyko-type equations in Table 1 follow a proportional relationship, that is, E will experience a proportional change with a rate of α when P_j, PE_j, and S_c experience the same change rate

$$\alpha E_a = \alpha \sum_{j=1}^{3} f_g(P_j, PE_j, S_c, n_1, n_2) = \sum_{j=1}^{3} f_g(\alpha P_j, \alpha PE_j, \alpha S_c, n_1, n_2) \quad (22)$$

Substituting $\frac{1}{P_a}$, $\frac{1}{PE_a}$, and $\frac{1}{W_P}$ for α, we will obtain generalized Budyko equations in three dimensionless spaces, like the Buckingham-π theorem (Daly et al., 2019; Barenblatt et al., 1996).

$$\frac{E_a}{P_a} = \sum_{j=1}^{3} f_g(\frac{P_j}{P_a}, \frac{PE_j}{P_a}, \frac{S_c}{P_a}, n_1, n_2) \quad (23)$$

$$\frac{E_a}{PE_a} = \sum_{j=1}^{3} f_g(\frac{P_j}{PE_a}, \frac{PE_j}{PE_a}, \frac{S_c}{PE_a}, n_1, n_2) \quad (24)$$

$$\frac{E_a}{S_c} = \sum_{j=1}^{3} f_g(\frac{P_j}{S_c}, \frac{PE_j}{S_c}, 1, n_1, n_2) \quad (25)$$

Eqs. (23) to (25) are scaled by P_a, PE_a, and W_P, respectively. Yang-Yang equation is taken as an example to show the proportional relationship. The Yang-Yang equation is expressed as follows

$$E_a = \sum_{j=1}^{3}(((P_j^{-n_1} + S_c^{-n_1})^{-\frac{1}{n_1}})^{-n_2} + PE_j^{-n_2})^{-\frac{1}{n_2}} \quad (26)$$

Multiplying both sides by α, we obtain the proportional relationship

$$\alpha E_a = \sum_{j=1}^{3}((((\alpha P_j)^{-n_1} + (\alpha S_c)^{-n_1})^{-\frac{1}{n_1}})^{-n_2} + (\alpha PE_j)^{-n_2})^{-\frac{1}{n_2}} \quad (27)$$

3.2 Linkage to Budyko-type equation

Budyko-type equations are the foundations for generalization, and can be viewed as the special cases of generalized Budyko equations under uniform distribution of P and PE throughout the year and infinite S_c. Let us assume that

$$P_j = \frac{1}{3}P_a,\ PE_j = \frac{1}{3}PE_a, j = 1, 2, \text{and } 3 \quad (28)$$

Hydrology and Earth System Sciences
Discussions

$$S_c \rightarrow \infty \tag{29}$$

Based on uniform distribution of P and PE, we can rewrite E_a as 3 times of E_j

$$E_a = 3E_j = 3B_2(B_1(P_j, S_c, n_1), PE_j, n_2) = 3B_2(B_1\left(\frac{1}{3}P_a, S_c, n_1\right), \frac{1}{3}PE_a, n_2) \tag{30}$$

The proportional relationship further simplifies Eq. (30) as

$$E_a = B_2(B_1(P_a, 3S_c, n_1), PE_a, n_2) \tag{31}$$

Eq. (31) gives the form of generalized Budyko-type equations with the incorporation of storage limit (S_c) under uniform P and PE. The $3S_c$ in the right side of Eq. (31) is due to our assumption of three complete rainfall-runoff events in a hydrological year. If S_c tends to be infinite, the boundary condition in Budyko-type equations determines that $B_1(P_a, 3S_c, n_1) = P_a$ from Eq. (15) as $\frac{3S_c}{P_a} \rightarrow \infty$. Replacing $B_1(P_a, 3S_c, n_1)$ with P_a in Eq (31) gives that

$$E_a = B_2(P_a, PE_a, n_2) \tag{32}$$

Thus, generalized equation is simplified to the Budyko equation (i.e., Eq. (32)) with uniform distribution of P and PE and infinite S_c. Here, Yang-Yang equation is used as an example to explain this simplification. The expression of Yang-Yang equation is

$$E_a = \sum_{j=1}^{3}(((P_j{}^{-n_1} + S_c{}^{-n_1})^{-\frac{1}{n_1}})^{-n_2} + PE_j{}^{-n_2})^{-\frac{1}{n_2}} \tag{33}$$

The uniform distribution of P and PE determines that

$$E_a = (((P_a{}^{-n_1} + (3S_c)^{-n_1})^{-\frac{1}{n_1}})^{-n_2} + PE_a{}^{-n_2})^{-\frac{1}{n_2}} \tag{34}$$

If $S_c \rightarrow \infty$, The value $(3S_c)^{-n_1}$ approaches 0 and $((P_a{}^{-n_1} + (3S_c)^{-n_1})^{-\frac{1}{n_1}} \rightarrow P_a$. As a result, Yang-Yang equation is simplified as

$$E_a = (P_a{}^{-n_2} + PE_a{}^{-n_2})^{-\frac{1}{n_2}} \tag{35}$$

Eq. (35) is the same as Yang equation and n_2 corresponds to the parameter n in Yang equation (Yang et al., 2008). The simplification of other forms of generalized Budyko-type equations can be similarly derived following the above routine.

3.3 Values of $\frac{E_a}{P_a}$ in the generalized Budyko-type equations

The relationship between $\frac{E_a}{P_a}$ and $\frac{PE_a}{P_a}$ under different $\frac{S_c}{P_a}$, climate seasonality, and parameters (n_1 and n_2) using Yang-Yang equation are shown in Figure 2. The results using Yang-Fu, Fu-Yang, and Fu-Fu equations are provided in Figure S1 to S3. In general, E_a is similarly simulated in all four generalized Budyko-type equations, because Fu equation and Yang equation perform very similarly (Zhang et al., 2020; Zhou et al., 2015b; Andréassian and Sari, 2019). Here, Yang-Yang equation is used as an example for analysis.

The Figure 2a indicates that $\frac{E_a}{P_a}$ is positively correlated with $\frac{S_c}{P_a}$. Catchments with small water storage capacity (e.g., $\frac{S_c}{P_a} = 0.2$) cannot make $\frac{E_a}{P_a}$ approach to 1 despite infinite $\frac{PE_a}{P_a}$, and such a limit from S_c is ignored in Budyko-type equations. When S_c approaches to infinite (e.g., $\frac{S_c}{P_a} = 5$), the curve using Yang-Yang equation is the nearly same as Yang equation, and verify the simplification from generalized equations to Budyko-type equations with uniform climate and infinite S_c (black dashed lines in Figure 2a and c-f). The impacts of climate seasonality were demonstrated by the comparison of $\frac{E_a}{P_a}$ under uniform, in-phase, semi-uniform, and out-of-phase climates (Figure 2b). The temporal distribution of P_a to PE_a in these four climates are shown in Figure S4. Uniform climate refers to uniform P_a to PE_a, while semi-uniform climate has uniform P_a and seasonally changing PE_a. In-phase (out-of-phase) climate refers to synchronous (asynchronous) P_a and PE_a. Theoretical simulations suggest $\frac{E_a}{P_a}$ decreases from uniform, in-phase, semi-uniform, to out-of-phase climates under the same $\frac{PE_a}{P_a}$ and $\frac{S_c}{P_a}$ (Figure 2b). The simulated impacts of climate seasonality on $\frac{E_a}{P_a}$ are consistent with previous observations (Berghuijs et al., 2020; De Lavenne and Andréassian, 2018).

Two parameters (n_1 and n_2) mainly control the runoff yielding processes in two partitioning stages. Larger n_1 and n_2 lead to larger E_a, and thus n_1 and n_2 are positively correlated to $\frac{E_a}{P_a}$ in the generalized equations (Figure 2c-f). The comparison between Figure 2c and d shows that n_1 mainly determines the impacts of $\frac{S_c}{P_a}$ on $\frac{E_a}{P_a}$, and it is due to n_1 controls the first partitioning stage that include water storage. Similarly, n_2 determines the upper boundary condition when $\frac{S_c}{P_a}$ is large from the comparison between Figure 2c and e. In summary, S_c and climate seasonality, two factors that cause systematic errors in Budyko framework, are theoretically captured in our generalized Budyko-type equations. The simplifications of generalized equations to Budyko-type equation have been verified from simulated $\frac{E_a}{P_a}$ under uniform climate and infinite S_c (Figure 2a and c-f). The shape of generalized equations can be adjusted through two parameters to include other hydroclimatic attributes.

https://doi.org/10.5194/hess-2022-309
Preprint. Discussion started: 15 September 2022

Hydrology and Earth System Sciences
Discussions

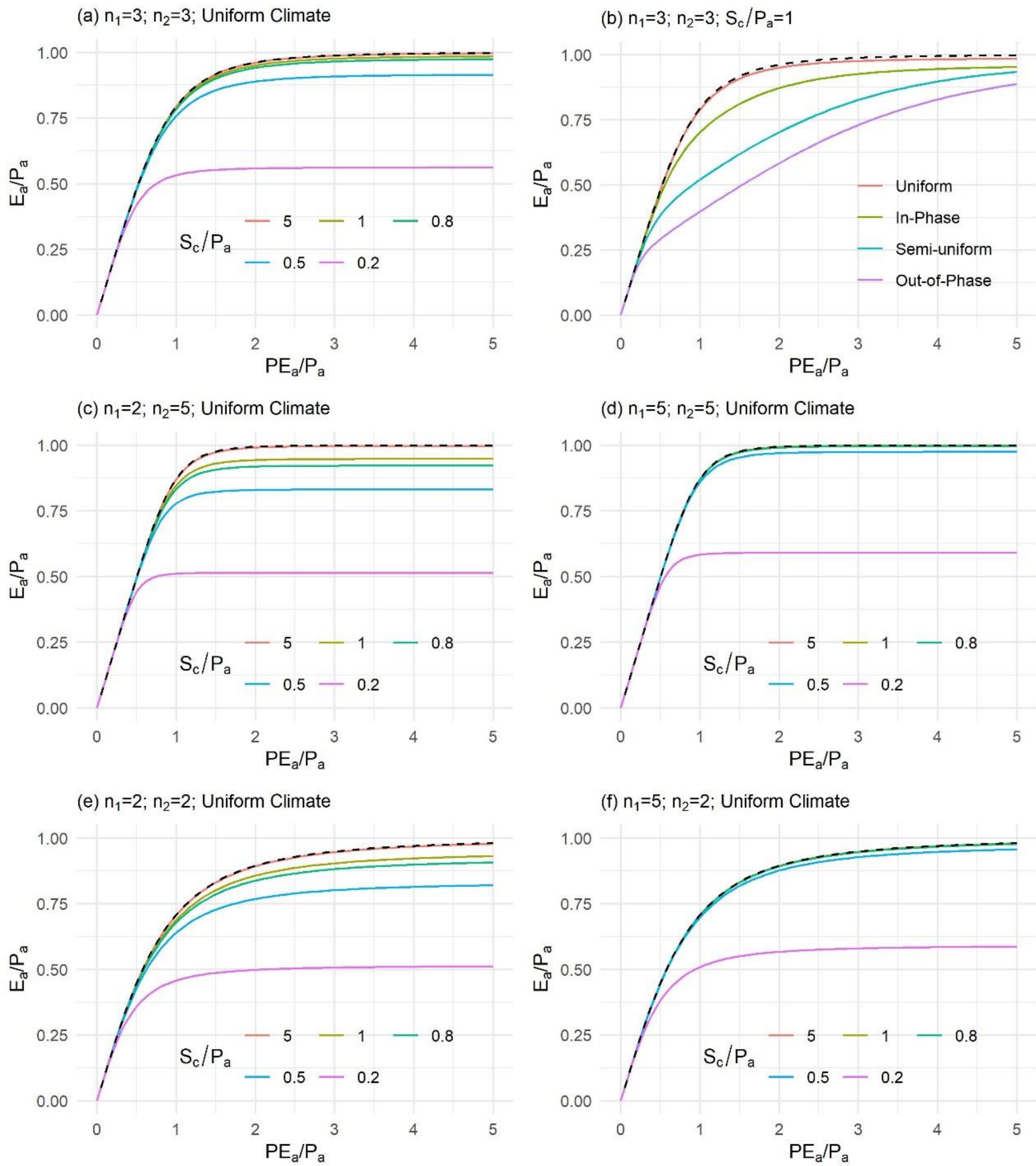

Figure 2 The $\frac{E_a}{P_a}$ versus $\frac{PE_a}{P_a}$ using Yang-Yang equation under different water storage capacity ($\frac{S_c}{P_a}$; a), climate seasonality (b), and parameters (n_1 and n_2; c-f). The values of parameters and climate seasonality are shown in titles. The black dashed lines represent simulated $\frac{E_a}{P_a}$ from Yang equation with its parameter equal to n_2.

275

4 Applications to the CONUS

4.1 Data

Our generalized Budyko-type equations were applied to the CONUS to demonstrate their necessity, physical interpretation, and performance. The P, PE, E, and S_c data in 671 catchments across the CONUS were collected from the catchment attributes and meteorology for large-sample studies (CAMELS) dataset (Addor et al., 2017; Newman et al., 2015). The mean 4-month P data were collected from the observations in Daymet dataset (Thornton et al., 2014), and mean 4-month PE data were estimated by the Priestly–Taylor method (Priestley and Taylor, 1972). R data were collected from the USGS National Water Information System server. Mean annual E is calculated as the difference between mean annual P and R based on water balance principles at the catchment scale in a long-term period. S_c is estimated as the product of soil depth and soil porosity in the unit of millimeter. The soil depth is collected from the P16 dataset as the depth of the permeable layers above bedrock (Pelletier et al., 2016). The soil porosity is computed from the sand and clay fractions from the State Soil Geographic Database (STATSGO), and is weighted by top nine soil layers and averaged over catchment scale (Miller and White, 1998; Addor et al., 2017).

Some catchments were eliminated in this study. First, the catchments where mean annual E is greater than P were not selected because it indicates the violation of water balance principle and model assumptions in this study. Second, the catchments with snow fraction >0.2 were not included in that snowmelt shows different hydrological properties from rainfall (Berghuijs et al., 2020; Berghuijs et al., 2014; Gnann et al., 2019), and models in this study do not consider snow dynamics. Finally, 471 catchments in the CONUS were selected to verify the generalized Budyko equations.

4.2 Necessity of incorporating water storage capacity and climate seasonality in Budyko framework

Apart from the theoretical and previously published evidence in the introduction part, here we used the hydrological data in CONUS to empirically demonstrate the necessity of incorporating climate seasonality and S_c in estimating E_a. Climate seasonality index (SI) in the CAMELS dataset is used to represent climate seasonality. SI is calculated from Eq. (14) in Woods (2009), and positive (negative) value indicates that P and PE are synchronous (asynchronous). Yang and Fu equations were applied to CONUS, and parameter n was estimated with the minimum squared errors between the observed and simulated E_a. The evaluation metrics are shown in Table 2, and Yang equation is used as an example (Figure 3). Similar to previous works (Berghuijs et al., 2020; De Lavenne and Andréassian, 2018; Potter et al., 2005), Budyko-type equations generally overestimate $\frac{E_a}{P_a}$ for catchments with out-of-phase climate and small S_c, and underestimate $\frac{E_a}{P_a}$ for in-phase climate and large S_c (Figure 3a, b). E_a and $\frac{E_a}{P_a}$ in some catchments are likely to be largely overestimated by Yang equation due to the loss of limits from water storage capacity and climate seasonality (Figure 3c-d). The errors in E_a, which are the difference between observed and simulated E_a, also show significantly negative correlation with SI and S_c, indicating their significance in controlling errors in Budyko framework (Figure 4). The results from Fu equation are very similar to those of Yang

https://doi.org/10.5194/hess-2022-309
Preprint. Discussion started: 15 September 2022

Hydrology and Earth System Sciences
Discussions

equation (Figure S5). Thus, physically incorporating climate seasonality and S_c into Budyko framework is necessary for future improvement. The negative impacts of SI and S_c to $\frac{E_a}{P_a}$ in observations are also consistent with the simulated results in generalized equations (Section 3.3), and validate our generalization.

Table 2 Parameters and evaluation metrics, including Pearson correlation coefficient (r) and coefficient of determination (r^2) for E_a and $\frac{E_a}{P_a}$, of the Budyko-type equations, generalized Budyko-type equation, and varying Budyko equations in the CONUS.

Type	Name	Parameters	Evaluation Metrics			
			$r\ (E_a)$	$r^2\ (E_a)$	$r\ (\frac{E_a}{P_a})$	$r^2\ (\frac{E_a}{P_a})$
Budyko-type equation	Yang	$n = 2.102$	0.787	0.616	0.889	0.771
	Fu	$n = 2.802$	0.789	0.619	0.890	0.773
Generalized Budyko-type equation	Yang -Yang	n_1 =7.288; n_2 =3.709	0.855	0.730	0.907	0.823
	Yang -Fu	n_1 =7.274; n_2 =4.422	0.854	0.730	0.907	0.822
	Fu - Yang	n_1 =7.990; n_2 =3.709	0.855	0.730	0.907	0.823
	Fu - Fu	n_1 =7.975; n_2 =4.423	0.854	0.730	0.907	0.822
Varying Budyko equations	Varying Yang	$\alpha_0 = 2.153; \alpha_1 = 0.206; \alpha_2 = 0.414$	0.842	0.709	0.905	0.814
	Varying Fu	$\alpha_0 = 2.857; \alpha_1 = 0.205; \alpha_2 = 0.409$	0.844	0.712	0.906	0.815

https://doi.org/10.5194/hess-2022-309
Preprint. Discussion started: 15 September 2022

Hydrology and Earth System Sciences
Discussions

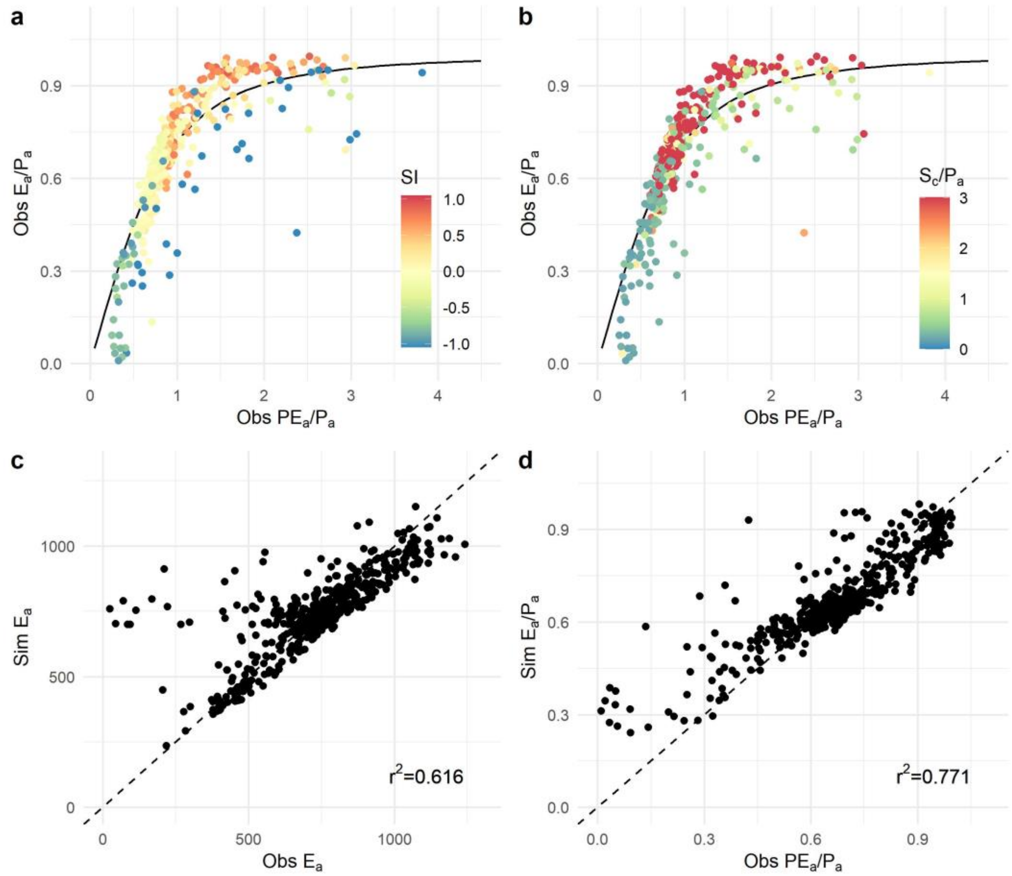

Figure 3 Applications of Yang equation to CONUS. (a-b) The observed pairs ($\frac{PE_a}{P_a}$ versus $\frac{E_a}{P_a}$; points) and their relationship to climate seasonality index (SI; a) and water storage capacity ($\frac{S_c}{P_a}$; b). Black lines are fitted Yang equations. (c-d) The comparison between simulated and observed E_a (c) and $\frac{E_a}{P_a}$ (d) using Yang equation. The black dashed lines are 1:1 lines with an intercept of 0.

320

https://doi.org/10.5194/hess-2022-309
Preprint. Discussion started: 15 September 2022

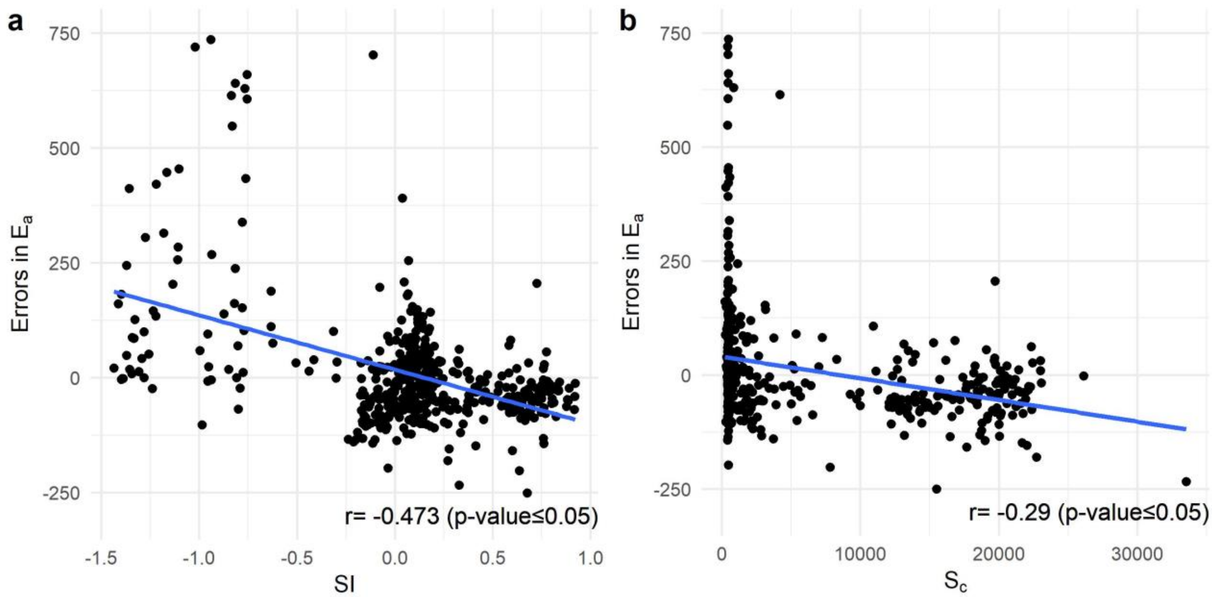

Figure 4 Relationships between the errors in E_a using Yang equation and climate seasonality index (SI; a) and water storage capacity (S_c; b). The Pearson correlation coefficient (r) and p-value are shown at bottom right. Blue lines are estimated from linear regression.

4.3 Performance of generalized Budyko-type equations

Four generalized Budyko-type equations were applied in the 471 catchments of CONUS to simulate E_a and $\frac{E_a}{P_a}$, and two parameters (n_1 and n_2) were estimated through the "L-BFGS-B" method (Byrd et al., 1995) with the minimum squared errors between the observed and simulated E_a. Estimated parameters (n_1 and n_2) and performance of generalized equations are shown in Table 2. All four equations achieve very similar performance, and we take Yang-Yang equation for an example. The r^2 for E_a and $\frac{E_a}{P_a}$ using Yang-Yang equation are 0.730 and 0.823, an improvement over Yang equation ($r^2 =$ 0.616 and 0.771 in Table 2). The comparison between simulated and observed $\frac{E_a}{P_a}$ and E_a shows that no systematic overestimation or underestimation exists in our simulation (Figure 5a, b). The simulated $\frac{E_a}{P_a}$ are positively correlated to SI and S_c (Figure 5c, d), and are in accord with the observation (Figure 3a, b). The errors in simulated E_a from Yang-Yang equation do not show significant correlation with SI and S_c (Figure 6), indicating that the systematic errors of E_a in Budyko-type equations due to climate seasonality and water storage capacity have been physically corrected by our generalization. Yang-Yang equation mainly decrease the errors in simulated E_a and $\frac{E_a}{P_a}$ for some catchments in the western and southeastern CONUS (Figure 7). These catchments have either asynchronous climate seasonality or shallow soil depth (Addor et al., 2017), showing that our generalized equations are able to be applied in the Mediterranean climate and catchments with small

https://doi.org/10.5194/hess-2022-309
Preprint. Discussion started: 15 September 2022

S_c. However, Yang-Yang equation increases the errors of simulated E_a and $\frac{E_a}{P_a}$ in Florida and some midwestern regions (Figure 7). The reason may be that soil depth and soil properties in the P16 and STATSGO dataset only consider the top 50m and 1.5m, which may not be accurate in these areas and induce errors for simulations. Meanwhile, our generalized equations bear errors for $\frac{E_a}{P_a}$ when SI= -1 (Figure 6c). Our generalization assumes that water storage change between 4-month intervals is zero, which ignore water inputs from antecedent soil moisture and may result in errors for catchments with asynchronous climate seasonality.

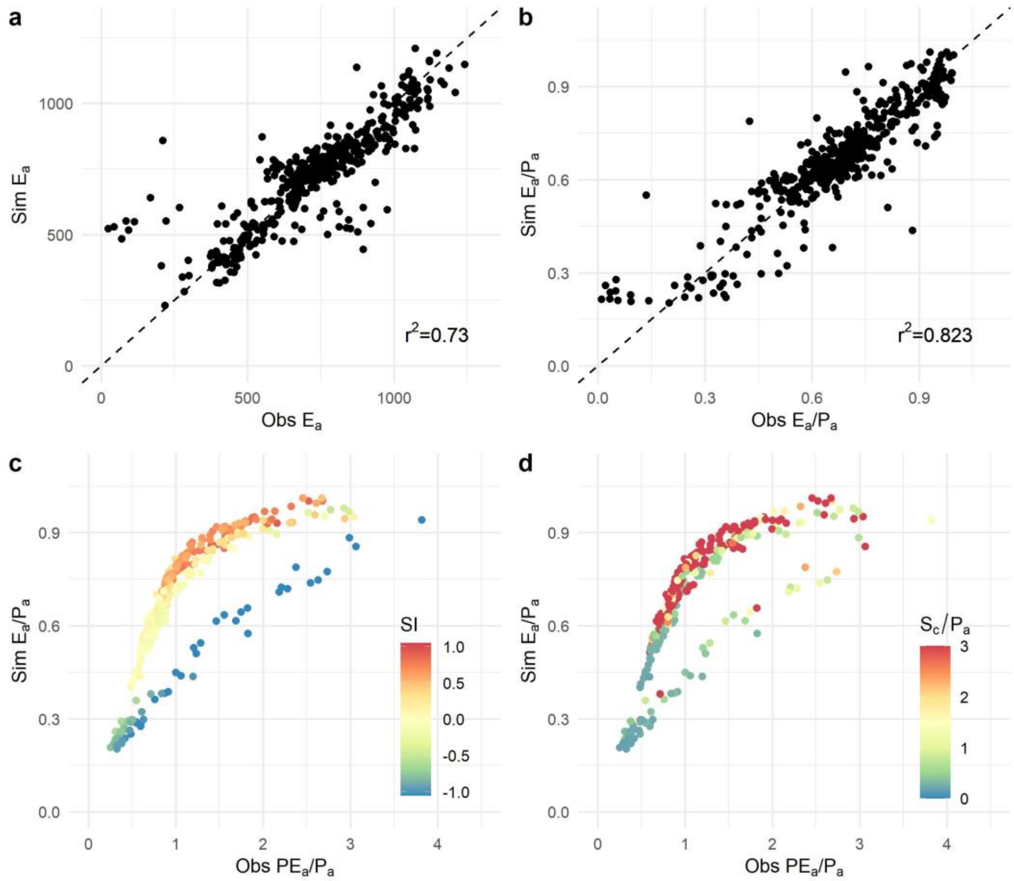

Figure 5 The performance of Yang-Yang equation in CONUS. (a-b) Comparison between simulated and observed E_a (a) and $\frac{E_a}{P_a}$ (b) from Yang-Yang equation. The black dashed lines are 1:1 lines with an intercept of 0. (c-d) The simulated $\frac{E_a}{P_a}$ versus observed $\frac{PE_a}{P_a}$ under different SI (c) and S_c/P_a (d).

https://doi.org/10.5194/hess-2022-309
Preprint. Discussion started: 15 September 2022

Hydrology and Earth System Sciences
Discussions

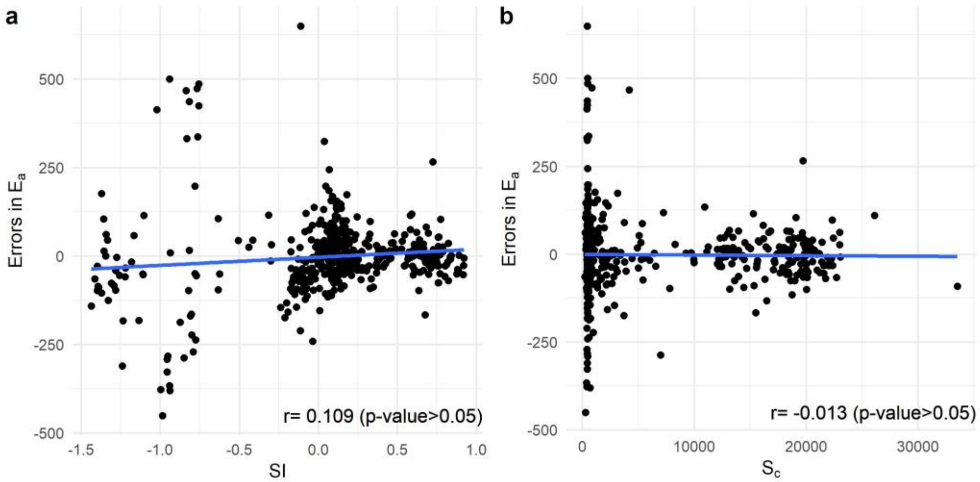

Figure 6 Relationship between the errors in simulated E_a using Yang-Yang equation and climate seasonality index (SI; a) and water storage capacity (S_c; b). The Pearson correlation coefficient (r) and related p-value are shown at bottom right. Blue lines are estimated from linear regression.

355

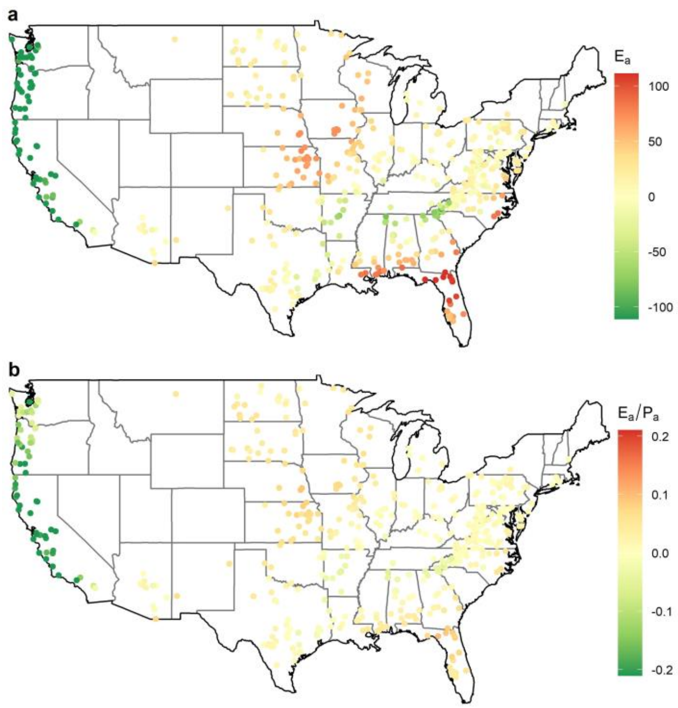

Figure 7 Difference of the errors in simulated E_a(a) and $\frac{E_a}{P_a}$ (b) between Yang-Yang equation and Yang equation

https://doi.org/10.5194/hess-2022-309
Preprint. Discussion started: 15 September 2022

4.4 Comparison with varying Budyko equation

Varying Budyko equation is a popular method to incorporate factors apart from P_a and PE_a in Budyko framework, where parameter n is linearly regressed to catchment properties (Zhang et al., 2019a; Zhang et al., 2019b; De Lavenne and Andréassian, 2018; Jiang et al., 2015). Here, normalized S_c ($x_{1,i}$) and SI ($x_{2,i}$), two factors that are incorporated in the generalized equations, were also used to explain the synthesized parameter (n_i) in varying Budyko equations

$$n_i = \alpha_0 + \alpha_1 x_{1,i} + \alpha_2 x_{2,i} \tag{36}$$

where n_i is the synthesized parameter in ith catchment; α_0, α_1, and α_2 are three regression parameters. The "L-BFGS-B" method is also used for parameters estimation with the minimum of squared errors between the observed and simulated E_a (Byrd et al., 1995).

The varying Yang equation and varying Fu equation were applied to CONUS, and achieve very similar performance as shown in Table 2. Take varying Yang equation as an example, the systematic overestimation is corrected and outliers in Budyko framework are captured by changing parameter n (Figure 8). However, the r^2 and r of varying Budyko equations are worse than those of generalized Budyko-type equations (Table 2), and varying Budyko equation has one more parameter than generalized Budyko-type equations. Meanwhile, three regression parameters (i.e., α_0, α_1, and α_2) in varying Budyko equation lack physical interpretation, and linear relationship deserves further examination. As a result, our generalized equations improve the accuracy and robustness for estimating long-term E with fewer parameters and provides additional physical interpretation compared with varying Budyko equations.

https://doi.org/10.5194/hess-2022-309
Preprint. Discussion started: 15 September 2022

Hydrology and Earth System Sciences
Discussions

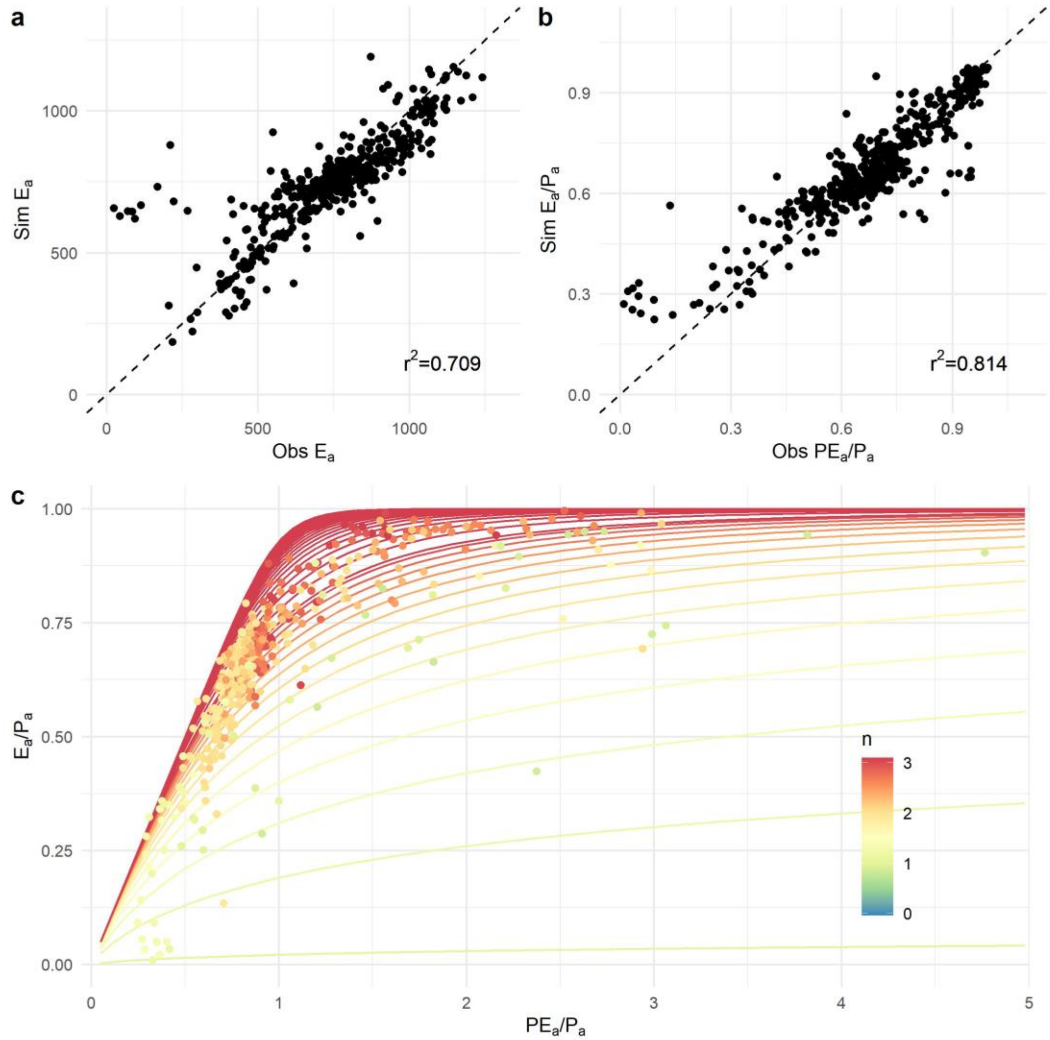

Figure 8 Performance of varying Yang equation in the CONUS. (a-b) The comparison between simulated and observed E_a (a) and $\frac{E_a}{P_a}$ (b). The black dashed lines are 1:1 lines with an intercept of 0. (c) The observed (points) and simulated (lines) $\frac{E_a}{P_a}$ versus observed $\frac{PE_a}{P_a}$ from varying Yang equation. The color represents the varying parameter n.

380 ## 5 Discussion

A generalized Budyko-type framework was proposed in this study to physically incorporate the impacts of climate seasonality and water storage in estimating E_a. The S_c is used as a new limiting variable that represents the maximum volume of water that can be saved in the catchment. Climate seasonality is included by modeling hydrological processes at a 4-month timescale. Thus, four factors (P, PE, S_c, and climate seasonality) were included in our generalized equations, and

https://doi.org/10.5194/hess-2022-309
Preprint. Discussion started: 15 September 2022

Hydrology and Earth System Sciences
Open Access
EGU
Discussions

each plays a distinct role. P measures available liquid water for evaporation; PE measures atmospheric demand and represents available energy to transform liquid water into water vapor; S_c measures the space where evaporation can occur; climate seasonality indicates the temporal coupling between climatic variables. Two parameters, n_1 and n_2, control the fast flow and baseflow separately. The shape and upper bound of the generalized equations can be adjusted with varying n_1 and n_2. The clear physical interpretation may make generalized equations more robust and physically interpretable than previous Budyko equations with either constant or varying parameters. Meanwhile, previous Budyko-type equations can be viewed as special cases of generalized Budyko equations under uniform P and PE and infinite water storage capacity.

The applications in the CONUS show that our generalized Budyko-type equations not only have one fewer parameter than varying Budyko equations, but also achieve higher correlation (r) and explained variance (r^2) for E_a and $\frac{E_a}{P_a}$. The simulated impacts of climate seasonality and water storage on $\frac{E_a}{P_a}$ from generalized equations are in accord with observations in CONUS, which highlight the necessity and validity of our generalization. In addition, previous studies statistically regress parameter n to climate index or hydrological characteristics, which usually assume a linear relationship between n and explanatory variables (Zhang et al., 2019a; Zhang et al., 2019b; De Lavenne and Andréassian, 2018; Jiang et al., 2015). This assumption deserves physical examination, and is not able to fully represent climatic conditions. For example, SI is equal to 0 in both uniform and semi-uniform climates (Woods, 2009), while these two climates have different E_a and $\frac{E_a}{P_a}$ based on our simulations (Figure 2 and 3). Physical accounts of these factors are more appropriate for future applications with intensifying human activities and climate change.

The generalization in this study assumes that annual hydrological processes consist of three 4-month rainfall-runoff events, and Ponce-Shetty is applied at each time interval. Apart from the rising-recession-depletion period in hydrograph, this assumption is based on previous applications of Ponce-Shetty model, in which the wetting potential, representing maximum values for annual W, is approximately three to four times greater than S_c in CONUS (Gnann et al., 2019; Sivapalan et al., 2011). Other timescales were also examined for generalized Budyko-type equations in Figure 9, and r^2 for E_a at 3-month, 2-month, and 1-month timescales are still better than those of Budyko equations. The generalized Budyko-type equation at the 1-month timescale assumes that annual hydrological processes consist of 12 independent monthly rainfall-runoff evens. However, the groundwater and baseflow may not be close to zero at the end of each month, and carrying water storage between time intervals cannot be ignored (Zhang et al., 2020). The generalized equation at the 12-month timescale assumes one complete rainfall-runoff event in a hydrological year, while water storage may be used several times by multiple rainfall events in a hydrological year. Thus, modeling long-term water balance at the 4-month timescale is the most suitable choice for generalized Budyko-type equations in CONUS, and achieves the best performance.

This study estimates S_c from observed soil depth and porosity, and does not require any calibration (Miller and White, 1998; Addor et al., 2017; Pelletier et al., 2016). Thus, the generalized equations provide an independent limit of E from a hydrological perspective, and increase the potential for predicting E_a at ungauged catchments. However, current observations of soil properties include certain uncertainty due to low information about deep soil layers, scale inadequacy, limited depth, and among others (Addor et al., 2017). For example, soil depth estimated from STATSGO dataset (Miller and White, 1998) and P16 dataset (Pelletier et al., 2016) differ a lot for catchments with soil depth>1.5m. Storage capacity data estimated from ground observations and remote sensing are inconsistent globally, which largely influence hydrological simulations (Mao and Liu, 2019). Accurately estimating soil properties is the key for improving the performance of generalized equations and facilitating their global applications in the future.

The generalized Budyko framework has great potentials in the areas where the Budyko-type equations have been successfully used, such as elasticity analysis, attribution of runoff change, groundwater analysis, hydrological shift, and model calibration (Istanbulluoglu et al., 2012; Wang et al., 2016; Wang and Zhou, 2016; Chen and Sivapalan, 2020; Gao et al., 2020; Greve et al., 2020; Zhang et al., 2019a; Wang and Hejazi, 2011; Chen et al., 2013). The better performance of the generalized framework in the CONUS indicates that it can provide more accurate results than previous Budyko-type equations. Proposing new methods that decompose the impacts of aridity index, climate seasonality, and storage capacity on E_a based on generalized equations may help us better detect and quantify the impacts of human activities and climate change on water resources.

Hydrology and Earth System Sciences
Open Access
Discussions

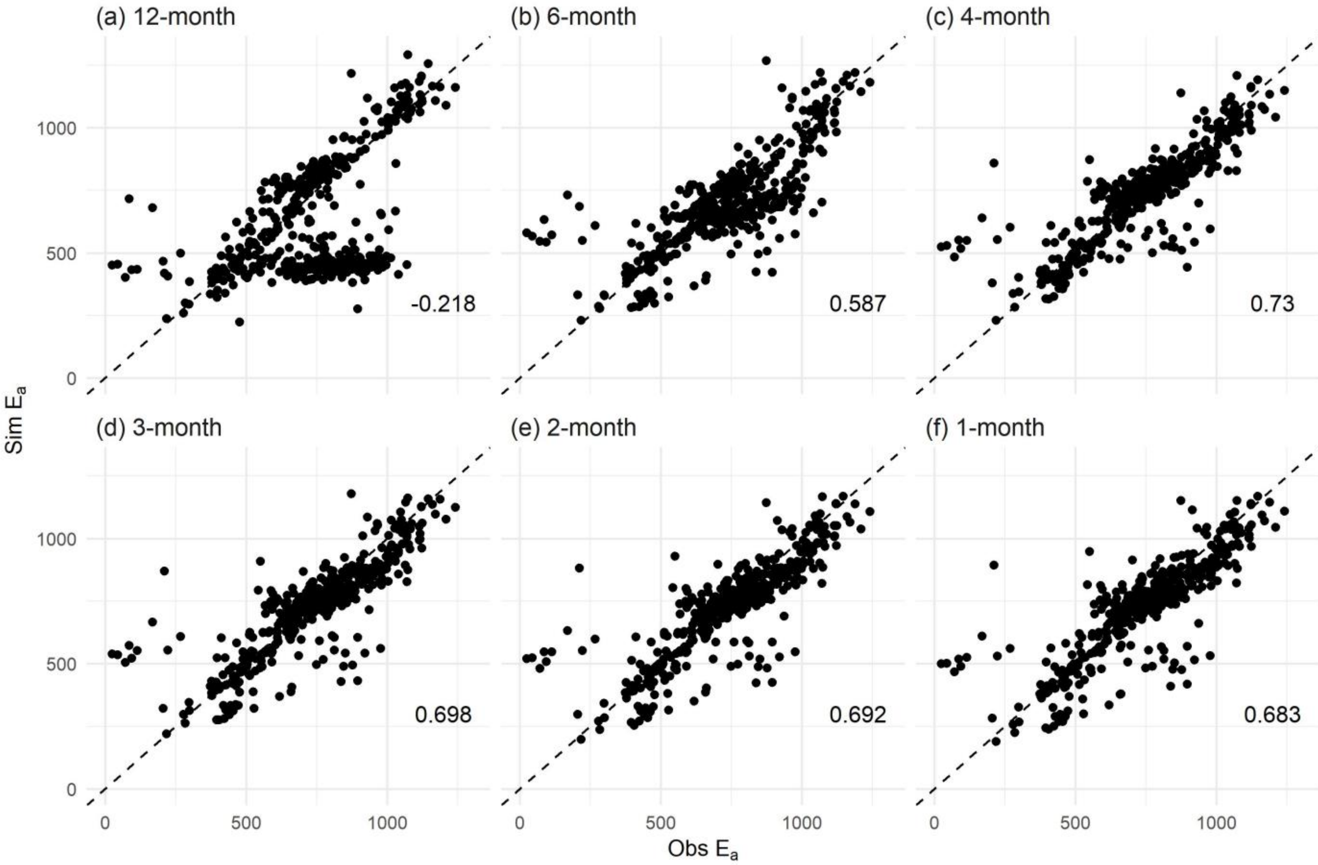

Figure 9 Comparison between simulated and observed E_a using Yang-Yang equation at various timescales. The numbers at bottom right are the coefficients of determination (r^2) for E_a.

435 **6 Conclusions**

In this study, a generalized Budyko framework was analytically proposed with physical accounts of climate seasonality and water storage capacity for simulating mean annual E. The S_c is introduced as a new explanatory variable to represent water storage capacity, and Ponce-Shetty model is used to model hydrological processes at a 4-month timescale. Previous Budyko-type equations can be treated as special cases with uniform climate and infinite S_c. The applications to the CONUS show that the incorporation of climate seasonality and water storage capacity is necessary in estimating E_a, and our generalized equations theoretically capture the observed impacts of these two factors. Meanwhile, the generalized equations perform better than previous varying Budyko equations and include one fewer parameter. Overall, the new framework represents an improvement over previous Budyko-type equations in terms of physical interpretation and accuracy. Further applications of the new framework in long-term water balance analysis are highly desirable.

Data availability

The hydrometeorological datasets and catchment attributes in the contiguous United States are provided by Newman et al. (2015) and Addor et al. (2017), and are available at https://ral.ucar.edu/solutions/products/camels.

Author contributions

XZ and RW conceived the original idea. XZ designed the overall study and wrote the first draft. JL and QD interpreted the results and supervised the progress. All authors contribute to the discussion and revision of manuscript.

Competing interests

The contact author has declared that none of the authors has any competing interests.

Acknowledgments

This research was supported by Hong Kong Research Grants Council (No. 17303017) and National Natural Science Foundation of China (No. 51979198).

References

Addor, N., Newman, A. J., Mizukami, N., and Clark, M. P.: The CAMELS data set: catchment attributes and meteorology for large-sample studies, Hydrol. Earth Syst. Sci., 21, 5293-5313, 10.5194/hess-21-5293-2017, 2017.

Andréassian, V. and Sari, T.: Technical Note: On the puzzling similarity of two water balance formulas – Turc–Mezentsev vs. Tixeront–Fu, Hydrol. Earth Syst. Sci., 23, 2339-2350, 10.5194/hess-23-2339-2019, 2019.

Arnold, J. G., Srinivasan, R., Muttiah, R. S., and Williams, J. R.: Large area hydrological modeling and assessment part I: model development Journal of the American Water Resources Association, 34, 73-89, 10.1111/j.1752-1688.1998.tb05961.x, 1998.

Barenblatt, G. I., Barenblatt, G. I., and Isaakovich, B. G.: Scaling, self-similarity, and intermediate asymptotics: dimensional analysis and intermediate asymptotics, Cambridge University Press1996.

Berghuijs, W. R., Gnann, S. J., and Woods, R. A.: Unanswered questions on the Budyko framework, Hydrological Processes, 1-5, 10.1002/hyp.13958, 2020.

Berghuijs, W. R., Woods, R. A., and Hrachowitz, M.: A precipitation shift from snow towards rain leads to a decrease in streamflow, Nature Climate Change, 4, 583-586, 2014.

Berghuijs, W. R., Larsen, J. R., van Emmerik, T. H. M., and Woods, R. A.: A Global Assessment of Runoff Sensitivity to Changes in Precipitation, Potential Evaporation, and Other Factors, Water Resources Research, 53, 8475-8486, 10.1002/2017WR021593, 2017.

Beven, K.: Prophecy, reality and uncertainty in distributed hydrological modelling, Advances in Water Resources, 16, 41-51, 10.1016/0309-1708(93)90028-E, 1993.

Bondy, J., Wienhöfer, J., Pfister, L., and Zehe, E.: Exploring the role of soil storage capacity for explaining deviations from the Budyko curve using a simple water balance model, Hydrol. Earth Syst. Sci. Discuss., 2021, 1-24, 10.5194/hess-2021-174, 2021.

Budyko, M. I.: Climate and life, New York:Academic Press1974.

Byrd, R. H., Lu, P., Nocedal, J., and Zhu, C.: A limited memory algorithm for bound constrained optimization, SIAM Journal on scientific computing, 16, 1190-1208, 1995.

Chen, X. and Sivapalan, M.: Hydrological Basis of the Budyko Curve: Data-Guided Exploration of the Mediating Role of Soil Moisture, Water Resources Research, 56, e2020WR028221, 10.1029/2020wr028221, 2020.

Chen, X., Alimohammadi, N., and Wang, D.: Modeling interannual variability of seasonal evaporation and storage change based on the extended Budyko framework, Water Resources Research, 49, 6067–6078, 2013.

Daly, E., Calabrese, S., Yin, J., and Porporato, A.: Hydrological Spaces of Long-Term Catchment Water Balance, Water Resources Research, 55, 10747-10764, 10.1029/2019wr025952, 2019.

de Lavenne, A. and Andréassian, V.: Impact of climate seasonality on catchment yield: A parameterization for commonly-used water balance formulas, Journal of Hydrology, 558, 266-274, 10.1016/j.jhydrol.2018.01.009, 2018.

Dunn, S. M., McDonnell, J. J., and Vaché, K. B.: Factors influencing the residence time of catchment waters: A virtual experiment approach, Water Resources Research, 43, 10.1029/2006WR005393, 2007.

Fu, B.: On The Calculation Of the Evaporation From Land Surface, Chinese Journal of Atmospheric Sciences, 5, 23-31, 1981.

Gao, F., Wang, H., and Liu, C.: Long-term assessment of groundwater resources carrying capacity using GRACE data and Budyko model, Journal of Hydrology, 588, 125042, 10.1016/j.jhydrol.2020.125042, 2020.

Gnann, S. J., Woods, R. A., and Howden, N. J. K.: Is there a baseflow Budyko curve?, Water Resources Research, 55, 17, 10.1029/2018WR024464, 2019.

Greve, P., Burek, P., and Wada, Y.: Using the Budyko Framework for Calibrating a Global Hydrological Model, Water Resources Research, 56, e2019WR026280, 10.1029/2019WR026280, 2020.

Greve, P., Gudmundsson, L., Orlowsky, B., and Seneviratne, S. I.: Introducing a probabilistic Budyko framework, Geophysical Research Letters, 42, 2261-2269, 10.1002/2015GL063449, 2015.

Gudmundsson, L., Greve, P., and Seneviratne, S. I.: The sensitivity of water availability to changes in the aridity index and other factors—A probabilistic analysis in the Budyko space, Geophysical Research Letters, 43, 6985-6994, 10.1002/2016GL069763, 2016.

Henley, B. J., Thyer, M. A., Kuczera, G., and Franks, S. W.: Climate-informed stochastic hydrological modeling: Incorporating decadal-scale variability using paleo data, Water Resources Research, 47, W11509, Artn W1150910.1029/2010wr010034, 2011.

Istanbulluoglu, E., Wang, T., Wright, O. M., and Lenters, J. D.: Interpretation of hydrologic trends from a water balance perspective: The role of groundwater storage in the Budyko hypothesis, Water Resources Research, 48, W00H16, 10.1029/2010wr010100, 2012.

Jiang, C., Xiong, L., Wang, D., Liu, P., Guo, S., and Xu, C. Y.: Separating the impacts of climate change and human activities on runoff using the Budyko-type equations with time-varying parameters, Journal of Hydrology, 522, 326-338, 2015.

Katsuyama, M., Tani, M., and Nishimoto, S.: Connection between streamwater mean residence time and bedrock groundwater recharge/discharge dynamics in weathered granite catchments, Hydrological Processes, 24, 2287-2299, 10.1002/hyp.7741, 2010.

Lan, T., Lin, K. R., Liu, Z. Y., He, Y. H., Xu, C. Y., Zhang, H. B., and Chen, X. H.: A Clustering Preprocessing Framework for the Subannual Calibration of a Hydrological Model Considering Climate-Land Surface Variations, Water Resources Research, 54, 10034-10052, 10.1029/2018WR023160, 2018.

Li, D., Pan, M., Cong, Z., Zhang, L., and Wood, E.: Vegetation control on water and energy balance within the Budyko framework, Water Resources Research, 49, 969-976, 10.1002/wrcr.20107, 2013.

Liu, Z., Cheng, L., Zhou, G., Chen, X., Lin, K., Zhang, W., Chen, X., and Zhou, P.: Global Response of Evapotranspiration Ratio to Climate Conditions and Watershed Characteristics in a Changing Environment, Journal of Geophysical Research: Atmospheres, 125, e2020JD032371, 10.1029/2020JD032371, 2020.

L′vovich, M. I.: World water resources and their future, American Geophysical Union1979.

Mao, G. and Liu, J.: WAYS v1: a hydrological model for root zone water storage simulation on a global scale, Geosci. Model Dev., 12, 5267-5289, 10.5194/gmd-12-5267-2019, 2019.

Martinez, G. F. and Gupta, H. V.: Toward improved identification of hydrological models: A diagnostic evaluation of

https://doi.org/10.5194/hess-2022-309
Preprint. Discussion started: 15 September 2022

the "abcd" monthly water balance model for the conterminous United States, Water Resources Research, 46, W08507, 10.1029/2009WR008294, 2010.

Mianabadi, A., Davary, K., Pourreza-Bilondi, M., and Coenders-Gerrits, A. M. J.: Budyko framework; towards non-steady state conditions, Journal of Hydrology, 588, 125089, 10.1016/j.jhydrol.2020.125089, 2020.

Miller, D. A. and White, R. A.: A Conterminous United States Multilayer Soil Characteristics Dataset for Regional Climate and Hydrology Modeling, Earth Interactions, 2, 1-26, 10.1175/1087-3562(1998)002<0001:ACUSMS>2.3.CO;2, 1998.

Milly, P. C. D.: An analytic solution of the stochastic storage problem applicable to soil water, Water Resources Research, 29, 3755-3758, 10.1029/93WR01934, 1993.

Milly, P. C. D.: Climate, soil water storage, and the average annual water balance, Water Resources Research, 30, 2143-2156, 10.1029/94WR00586, 1994.

Milly, P. C. D., Dunne, K. A., and Vecchia, A. V.: Global pattern of trends in streamflow and water availability in a changing climate, Nature, 438, 347-350, 10.1038/nature04312, 2005.

Moretti, G. and Montanari, A.: AFFDEF: A spatially distributed grid based rainfall–runoff model for continuous time simulations of river discharge, Environmental Modelling & Software, 22, 823-836, 10.1016/j.envsoft.2006.02.012, 2007.

Newman, A. J., Clark, M. P., Sampson, K., Wood, A., Hay, L. E., Bock, A., Viger, R. J., Blodgett, D., Brekke, L., Arnold, J. R., Hopson, T., and Duan, Q.: Development of a large-sample watershed-scale hydrometeorological data set for the contiguous USA: data set characteristics and assessment of regional variability in hydrologic model performance, Hydrol. Earth Syst. Sci., 19, 209-223, 10.5194/hess-19-209-2015, 2015.

Ning, T., Zhou, S., Chang, F., Shen, H., Li, Z., and Liu, W.: Interaction of vegetation, climate and topography on evapotranspiration modelling at different time scales within the Budyko framework, Agricultural and Forest Meteorology, 275, 59-68, 10.1016/j.agrformet.2019.05.001, 2019.

Oki, T. and Kanae, S.: Global Hydrological Cycles and World Water Resources, Science, 313, 1068-1072, 10.1126/science.1128845, 2006.

Pelletier, J. D., Broxton, P. D., Hazenberg, P., Zeng, X., Troch, P. A., Niu, G.-Y., Williams, Z., Brunke, M. A., and Gochis, D.: A gridded global data set of soil, intact regolith, and sedimentary deposit thicknesses for regional and global land surface modeling, Journal of Advances in Modeling Earth Systems, 8, 41-65, 10.1002/2015MS000526, 2016.

Ponce, V. M. and Shetty, A. V.: A conceptual model of catchment water balance: 1. Formulation and calibration, Journal of Hydrology, 173, 27-40, 10.1016/0022-1694(95)02739-C, 1995.

Porporato, A., Daly, E., and Rodriguez‐Iturbe, I.: Soil Water Balance and Ecosystem Response to Climate Change, The American Naturalist, 164, 625-632, 10.1086/424970, 2004.

Potter, N. J., Zhang, L., Milly, P. C. D., McMahon, T. A., and Jakeman, A. J.: Effects of rainfall seasonality and soil moisture capacity on mean annual water balance for Australian catchments, Water Resources Research, 41, 10.1029/2004WR003697, 2005.

Priestley, C. H. B. and Taylor, R. J.: On the assessment of surface heat flux and evaporation using large-scale parameters, Monthly weather review, 100, 81-92, 1972.

Reaver, N. G. F., Kaplan, D. A., Klammler, H., and Jawitz, J. W.: Theoretical and empirical evidence against the Budyko catchment trajectory conjecture, Hydrol. Earth Syst. Sci., 26, 1507-1525, 10.5194/hess-26-1507-2022, 2022.

Rodriguez-Iturbe, I., Porporato, A., Ridolfi, L., Isham, V., and Coxi, D. R.: Probabilistic modelling of water balance at a point: the role of climate, soil and vegetation, Proceedings of the Royal Society of London. Series A: Mathematical, Physical and Engineering Sciences, 455, 3789-3805, 10.1098/rspa.1999.0477, 1999.

Sankarasubramanian, A. and Vogel, R. M.: Annual hydroclimatology of the United States, Water Resources Research, 38, 1083, 2002.

Sivapalan, M., Yaeger, M. A., Harman, C. J., Xu, X., and Troch, P. A.: Functional model of water balance variability at the catchment scale: 1. Evidence of hydrologic similarity and space-time symmetry, Water Resources Research, 47, 10.1029/2010wr009568, 2011.

Thornton, P. E., Thornton, M. M., Mayer, B. W., Wilhelmi, N., Wei, Y., Devarakonda, R., and Cook, R. B.: Daymet: Daily Surface Weather Data on a 1-km Grid for North America, Version 2, 10.3334/ORNLDAAC/1219, 2014.

Vitvar, T., Burns, D. A., Lawrence, G. B., McDonnell, J. J., and Wolock, D. M.: Estimation of baseflow residence times in watersheds from the runoff hydrograph recession: method and application in the Neversink watershed, Catskill Mountains,

https://doi.org/10.5194/hess-2022-309
Preprint. Discussion started: 15 September 2022

New York, Hydrological Processes, 16, 1871-1877, 10.1002/hyp.5027, 2002.

Vörösmarty, C. J., McIntyre, P. B., Gessner, M. O., Dudgeon, D., Prusevich, A., Green, P., Glidden, S., Bunn, S. E., Sullivan, C. A., Liermann, C. R., and Davies, P. M.: Global threats to human water security and river biodiversity, Nature, 467, 555-561, 10.1038/nature09440, 2010.

Wang, C., Wang, S., Fu, B., and Zhang, L.: Advances in hydrological modelling with the Budyko framework:A review, Progress in Physical Geography: Earth and Environment, 40, 409-430, 10.1177/0309133315620997, 2016.

Wang, D. and Hejazi, M.: Quantifying the relative contribution of the climate and direct human impacts on mean annual streamflow in the contiguous United States, Water Resources Research, 47, 10.1029/2010WR010283, 2011.

Wang, D. and Tang, Y.: A one-parameter Budyko model for water balance captures emergent behavior in darwinian hydrologic models, Geophysical Research Letters, 41, 4569-4577, 10.1002/2014GL060509, 2014.

Wang, D., Zhao, J., Tang, Y., and Sivapalan, M.: A thermodynamic interpretation of Budyko and L'vovich formulations of annual water balance: Proportionality Hypothesis and maximum entropy production, Water Resources Research, 51, 3007-3016, 10.1002/2014WR016857, 2015.

Wang, X. S. and Zhou, Y.: Shift of annual water balance in the Budyko space for catchments with groundwater-dependent evapotranspiration, Hydrol. Earth Syst. Sci., 20, 3673-3690, 10.5194/hess-20-3673-2016, 2016.

Westra, S., Thyer, M., Leonard, M., Kavetski, D., and Lambert, M.: A strategy for diagnosing and interpreting hydrological model nonstationarity, Water Resources Research, 50, 5090-5113, 10.1002/2013WR014719, 2014.

Woods, R.: The relative roles of climate, soil, vegetation and topography in determining seasonal and long-term catchment dynamics, Advances in Water Resources, 26, 295-309, 10.1016/S0309-1708(02)00164-1, 2003.

Woods, R. A.: Analytical model of seasonal climate impacts on snow hydrology: Continuous snowpacks, Advances in Water Resources, 32, 1465-1481, 10.1016/j.advwatres.2009.06.011, 2009.

Wu, C., Hu, B. X., Huang, G., and Zhang, H.: Effects of climate and terrestrial storage on temporal variability of actual evapotranspiration, Journal of Hydrology, 549, 388-403, 10.1016/j.jhydrol.2017.04.012, 2017.

Wu, C., Yeh, P. J.-F., Hu, B. X., and Huang, G.: Controlling factors of errors in the predicted annual and monthly evaporation from the Budyko framework, Advances in Water Resources, 121, 432-445, 2018a.

Wu, C., Yeh, P. J. F., Hu, B. X., and Huang, G.: Controlling factors of errors in the predicted annual and monthly evaporation from the Budyko framework, Advances in Water Resources, 121, 432-445, 10.1016/j.advwatres.2018.09.013, 2018b.

Yang, D., Shao, W., Yeh, P. J.-F., Yang, H., Kanae, S., and Oki, T.: Impact of vegetation coverage on regional water balance in the nonhumid regions of China, Water Resources Research, 45, W00A14, 10.1029/2008wr006948, 2009.

Yang, D., Sun, F., Liu, Z., Cong, Z., Ni, G., and Lei, Z.: Analyzing spatial and temporal variability of annual water - energy balance in nonhumid regions of China using the Budyko hypothesis, Water Resources Research, 43, 436-451, 2007.

Yang, H., Choi, H. T., and Lim, H.: Applicability Assessment of Estimation Methods for Baseflow Recession Constants in Small Forest Catchments, Water, 10, 1074, 2018.

Yang, H., Yang, D., Lei, Z., and Sun, F.: New analytical derivation of the mean annual water-energy balance equation, Water Resources Research, 44, W034103, 10.1029/2007WR006135, 2008.

Zhang, L., Potter, N., Hickel, K., Zhang, Y., and Shao, Q.: Water balance modeling over variable time scales based on the Budyko framework – Model development and testing, Journal of Hydrology, 360, 117-131, 10.1016/j.jhydrol.2008.07.021, 2008.

Zhang, L., Hickel, K., Dawes, W. R., Chiew, F. H. S., Western, A. W., and Briggs, P. R.: A rational function approach for estimating mean annual evapotranspiration, Water Resources Research, 40, 1-14, 10.1029/2003wr002710, 2004.

Zhang, X., Dong, Q., Cheng, L., and Xia, J.: A Budyko-based framework for quantifying the impacts of aridity index and other factors on annual runoff, Journal of Hydrology, 579, 124224, 10.1016/j.jhydrol.2019.124224, 2019a.

Zhang, X., Dong, Q., Costa, V., and Wang, X.: A hierarchical Bayesian model for decomposing the impacts of human activities and climate change on water resources in China, Science of The Total Environment, 665, 836-847, 10.1016/j.scitotenv.2019.02.189, 2019b.

Zhang, X., Dong, Q., Zhang, Q., and Yu, Y.: A unified framework of water balance models for monthly, annual, and mean annual timescales, Journal of Hydrology, 589, 125186, 10.1016/j.jhydrol.2020.125186, 2020.

Zhao, J., Wang, D., Yang, H., and Sivapalan, M.: Unifying catchment water balance models for different time scales through the maximum entropy production principle, Water Resources Research, 52, 7503-7512, 10.1002/2016WR018977, 2016.

Zhou, G., Wei, X., Chen, X., Zhou, P., Liu, X., Xiao, Y., Sun, G., Scott, D. F., Zhou, S., Han, L., and Su, Y.: Global pattern for the effect of climate and land cover on water yield, Nature Communications, 6, 5918, 10.1038/ncomms6918, 2015a.

Zhou, S., Yu, B., Huang, Y., and Wang, G.: The complementary relationship and generation of the Budyko functions, Geophysical Research Letters, 42, 1781-1790, 10.1002/2015gl063511, 2015b.